

Tropical Journal of Natural Product Research

Available online at <https://www.tjnpr.org>

Original Research Article

Molecular Mechanism of *Avicennia marina* (Forssk.) Vierh. in Inhibiting Hepatitis C Virus Based on Network Pharmacology and Molecular Docking

Muhammad Arba^{1*}, Sunandar Ihsan¹, Nurul Fatihah¹, Jamili Jamili²¹Department of Pharmaceutical Analysis and Medicinal Chemistry, Faculty of Pharmacy, Universitas Halu Oleo, Kendari, Indonesia²Department of Biology, Faculty of Science, Universitas Halu Oleo, Kendari, Indonesia

ARTICLE INFO

Article history:

Received 19 January 2025

Revised 07 February 2025

Accepted 03 March 2025

Published online 01 May 2025

ABSTRACT

Hepatitis C virus (HCV) infection is a significant threat to human health, with a high prevalence in various countries around the world. To reduce its prevalence, natural resources have been reported to provide diverse structures and fewer side effects for developing anti-HCV treatments. Therefore, this study aims to assess the potential of *Avicennia Marina* (Forssk.) Vierh. (AM) to inhibit HCV infection using network pharmacology and molecular docking methods. The results identified the presence of 12 compounds and 11 core targets, including SRC, AKT1, tumor necrosis factor- α (TNF- α), HSP90AA1, EGFR, BCL2, JUN, PI3KCA, ESR1, CASP3, and HIF1A. In addition, 5 key targets, SRC, AKT1, TNF, HSP90AA1, and ESR1, met the criteria for Degree, Closeness, and Centrality. Molecular docking revealed that several compounds had lower binding energy than native ligands when bound to AKT1, TNF- α , and HSP90AA1. Avicennone D effectively inhibited AKT1 (binding energy of -7.074 kcal/mol) and TNF- α (binding energy of -5.282 kcal/mol), while Avicenol C and Avicennone F showed strong potentials against TNF- α (binding energy of each -6.151 kcal/mol and -5.622 kcal/mol, respectively) and HSP90AA1 (binding energy of each -10.369 kcal/mol and -9.525 kcal/mol, respectively). The inhibition results showed that Stenopquinone B had the potential to inhibit TNF- α (binding energy of -6.030 kcal/mol). A total of 10 compounds, including Avicenol A, Avicenol C, Avicenone A, Avicenone C, and Avicennone A-G, demonstrated comparable or superior binding energy to the native ligand for HSP90AA1. This study provided insights into molecular mechanisms through which AM could treat HCV infections by targeting key proteins.

Keywords: Hepatitis C virus, *Avicennia marina*, Network pharmacology, Tumor necrosis factor, Diabetes.

Introduction

Hepatitis C virus (HCV) is a widespread infectious disease affecting 0.5% to 4% of the world's population and has a significant risk of progressing to chronic conditions.¹ To reduce its prevalence, several studies have proposed the use of mangrove plants, which are rich in secondary metabolites and have been traditionally used to treat leprosy, ulcers, and malaria. In addition, mangrove-derived compounds have been reported to exhibit diverse biological activities, including antioxidant, antimicrobial, and antiviral effects.

Avicennia marina (AM), a mangrove species, is a known source of bioactive compounds, including flavonoids, tannins, steroids, and alkaloids. Extracts from AM have demonstrated several pharmacological effects, including anticancer, antibacterial, antifungal, and antiviral.²⁻³ Zandi et al. (2008) also demonstrated its efficacy against herpes simplex virus type 1 (HSV-1) and poliovirus *in vitro*.⁴

*Corresponding author. E mail: muh.arba@uho.ac.id

Tel.: +628114056877

Citation: Arba M, Ihsan S, Fatihah N, Jamili J. Molecular Mechanism of *Avicennia marina* (Forssk.) Vierh. in Inhibiting Hepatitis C Virus Based on Network Pharmacology and Molecular Docking. Trop J Nat Prod Res. 2025; 9(4): 1449 – 1456. <https://doi.org/10.26538/tjnpr/v9i4.10>

Official Journal of Natural Product Research Group, Faculty of Pharmacy, University of Benin, Benin City, Nigeria

Betulinic acid obtained from AM has shown antiviral activity against HCV by inhibiting Cyclooxygenase-2 (COX-2) expression through Nuclear Factor kappa-light-chain-enhancer of activated B cells (NF- κ B) and Mitogen-Activated Protein Kinase - Extracellular Signal-Regulated Kinase 1/2 (MAPK-ERK1/2) pathways.⁵ In addition, Devi et al. (2014) reported antibacterial activity of *A. marina* leaves against bacteria responsible for urinary tract infections.⁶ Behbahani et al. (2013) demonstrated the presence of antihelminthic compounds and reverse transcriptase enzyme inhibition in the crude methanol extract of AM leaves.⁷⁻⁸ Studies by Kathiresan et al. (2020) and Premnathan et al. (1992) also emphasized the antiviral properties of the leaves against hepatitis B virus and Newcastle disease virus.⁹⁻¹⁰

Despite the evidence of antiviral activity in AM, detailed studies on its interaction with HCV at molecular level in the multidrug multitarget paradigm are limited. In this study, network pharmacology and molecular docking methods are considered to investigate the potential of AM to inhibit HCV infection. Network pharmacology offers a systematic method to understanding the complex interactions between plant compounds and biological systems. Compared to the common "one-drug, one-target" paradigm, it embraces a multi-target strategy, recognizing that plant compounds often exert therapeutic effects through multiple pathways.¹¹⁻¹⁴

This method enables the construction of comprehensive networks of compound-target-disease relationships.¹⁵⁻¹⁶ By constructing compound-target-disease relationships, key molecular targets and the underlying mechanisms by which *A. marina* exerts its therapeutic effects are identified.

Molecular docking is a computational technique that predicts binding affinity and interaction patterns between small molecules and target proteins at the atomic level.¹⁷ By simulating molecular interactions, docking studies provide insights into the structural basis of ligand-

receptor binding, prioritizing potential compounds for further experimental validation. The combination of network pharmacology and molecular docking enabled the identification of bioactive compounds in AM with high specificity and affinity for HCV-relevant targets.

Materials and Methods

Drug-likeness Prediction

For simplification, the name *Avicennia marina* (Forssk.) Vierh was abbreviated as AM.

The bioactive compounds in AM were retrieved from Knapsack database (<http://www.knapsackfamily.com/KNAPSAcK>). Subsequently, drug-likeness properties of each compound were assessed using SwissADME web server (<http://www.swissadme.ch/>),¹⁸ in which SMILE codes for the compounds were input to determine their properties.

Genes identification associated with Hepatitis C virus (HCV)

In this study, target prediction for AM compounds was conducted using SwissTargetPrediction and SEA databases (<https://sea.bkslab.org>) with SMILE codes of each compound as input.¹⁹⁻²⁰ Genes linked to T2DM were identified through OMIM (<https://www.omim.org>) and GeneCard (<https://www.genecards.org>) databases,²¹⁻²² with GeneCard results refined to the top 500 targets.²³ The disease-related and compound-associated targets were then filtered and merged into a Venn diagram using the Bioinformatics and System Biology tool (<https://bioinformatics.psb.ugent.be/webtools/Venn>).

Protein-Protein Interaction (PPI) Network and Core Target Selection
Protein-protein interaction (PPI) network was constructed using STRING database (<https://string-db.org>), with the protein targets restricted to "Homo sapiens" and a high-confidence score of 0.007, while other parameters remained at default settings. Furthermore, the resulting PPI network was imported into Cytoscape v3.10.2 for further analysis.²⁴

GO Analysis and KEGG Path

Gene Ontology (GO) analysis was conducted using the Metascape (<https://www.metascape.org>) and shinyGO 0.80 databases to assess the biological functions, cellular processes, and molecular components of the predicted protein targets.²⁵⁻²⁷ Kyoto Encyclopedia of Genes and Genomes (KEGG) pathway analysis identified metabolic and molecular signals influenced by the compounds and targets of AM and HCV. These pathways were subsequently regarded as the active mechanisms of the compounds.

Table 1: Drug-likeness properties of all compounds were analyzed, with compounds violating more than one of Lipinski's Rule of Five emphasized in red.

No	Compound	Molecular Formula	Lipinski Rule of 5	MW (g/mol)	MlogP	Hbond Acceptor	Hbond Donor
1	Betaine	C ₅ H ₁₁ NO ₂	0 violation	117.15	-3.67	2	0
2	Luteorin 5-methyl ether 3'-glucoside	C ₂₂ H ₂₂ O ₁₁	2 violations	462.40	-1.89	11	6
3	Avicenol A	C ₁₇ H ₂₀ O ₅	0 violation	304.34	1.05	5	2
4	Avicenol C	C ₁₇ H ₂₀ O ₄	0 violation	288.34	1.88	4	1
5	Avicequinone A	C ₁₅ H ₁₄ O ₅	0 violation	274.27	-0.28	5	2
6	Avicequinone C	C ₁₅ H ₁₂ O ₄	0 violation	256.25	0.43	4	1
7	Avicennone A	C ₁₇ H ₂₀ O ₆	0 violation	320.34	1.29	6	1
8	Avicennone B	C ₁₇ H ₂₀ O ₇	0 violation	336.34	0.49	7	2
9	Avicennone C	C ₁₅ H ₁₆ O ₃	0 violation	244.29	1.48	3	1
10	Avicennone D	C ₁₂ H ₆ O ₄	0 violation	214.17	-0.10	4	1
11	Avicennone F	C ₁₅ H ₁₈ O ₄	0 violation	262.30	0.71	4	2
12	Avicennone G	C ₁₅ H ₁₈ O ₅	0 violation	278.30	-0.12	5	3
13	Stenocarpoquinone B	C ₁₅ H ₁₄ O ₄	0 violation	258.27	0.55	4	1
14	Marinoid A	C ₂₅ H ₃₀ O ₁₁	2 violations	506.50	-0.37	11	5
15	Marinoid B	C ₂₆ H ₃₂ O ₁₂	2 violations	536.53	-1.06	12	5
16	Marinoid C	C ₂₅ H ₃₀ O ₁₂	2 violations	522.50	-0.86	12	6
17	Marinoid D	C ₂₅ H ₃₀ O ₁₄	2 violations	554.50	-1.55	14	6

Molecular Docking

Molecular docking was carried out for the top 5 targets using the protein structures of SRC, AKT1, tumor necrosis factor (TNF), HSP90AA1, and ESR1 obtained from Protein Data Bank (PDB) database (<https://www.rcsb.org>). The 2D structures of AM compounds retrieved from Knapsack database were converted into 3D formats using the Maestro LigPrep Module with OPLS_2005 forcefield, where possible ionization states, tautomers, and stereoisomers were generated.²⁸⁻²⁹ Protein and ligand preparations followed established protocols and were conducted through the Maestro Schrödinger software (version 11.1.012, 2017-1 release, Schrödinger, New York, NY, USA).²⁸⁻²⁹ Initially, the target protein was retrieved from PDB and prepared using the Protein Preparation Wizard. This included assigning bond orders, adding hydrogen atoms, optimizing protonation states with Epik at physiological pH, and performing restrained energy minimization using OPLS4 force field. The water molecules were removed to prevent interference during docking protocol, while the receptor grid was generated by defining binding site based on the co-crystallized ligand. Docking was performed using Glide in extra precision (XP) mode for the most accurate ligand ranking. The docked complexes were analyzed based on the scores, with lower scores indicating better binding affinities. Ligand-protein interactions, such as hydrogen bonds, hydrophobic contacts, and π - π stacking, were visualized using the Ligand Interaction Diagram. The best-ranked ligand-protein complexes were selected for further analysis, and all docking results were compiled for comparative evaluation. Furthermore, the native ligands 821, OXZ, 307, P54, and RL4 were used as reference compounds for docking to SRC, AKT1, TNF, HSP90AA1, and ESR1, respectively. A redocking experiment was performed to validate the protocol by re-docking the co-crystallized ligand into the active site of the receptor and comparing the predicted pose with the experimental crystallographic pose. The co-crystallized ligand was extracted from the protein complex and prepared separately using LigPrep to generate the relevant ionization states and stereoisomers.

Results and Discussion

AM compounds were obtained from the Knapsack database, identifying a total of 17 compounds (Table 1).

Drug-likeness properties of the 17 compounds were evaluated, as presented in Table 1. Based on Lipinski's Rule of 5 criteria, compounds that violated more than 1 rule were excluded from further analysis. A total of 5 compounds, namely Luteorin 5-methyl ether 3'-glucoside, Marinoid A, Marinoid B, Marinoid C, and Marinoid D, did not meet the criteria and were emphasized in red. Consequently, only 12 compounds were selected for the subsequent network pharmacology studies.

The Target Genes of AM Compounds and HCV

The targets identified for AM compounds from SwissTargetPrediction, SEA, and TargetNet databases included 341, 223, and 1,622, respectively. For HCV, gene targets were retrieved from the GeneCards, DisGeNet, and OMIM databases, amounting to 500, 1,769, and 214, respectively. After eliminating duplicates, 1,055 targets for AM were consolidated from SwissTargetPrediction, SEA, and TargetNet, while 1,770 targets for HCV were refined from GeneCards, DisGeNet, and OMIM. A Venn diagram (Figure 1) revealed 182 overlapping common targets for AM and HCV.

PPI analysis was performed by STRING database (<http://string-db.org>) and visualized using Cytoscape v3.10.2 (<https://cytoscape.org>). Proteins with the highest interaction counts were identified, as displayed in Figure 2.

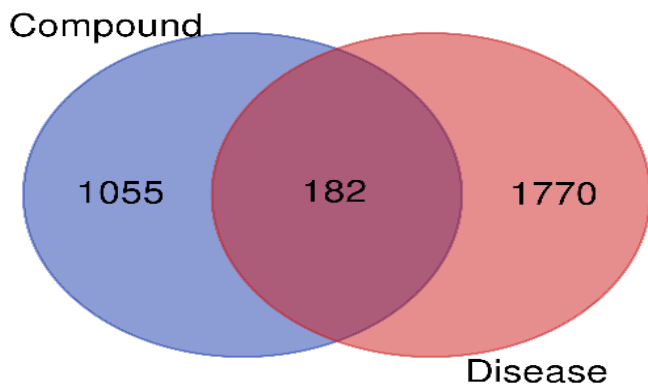


Figure 1: A Venn diagram illustrating the overlap between HCV and AM targets. Blue represented targets associated with AM compounds, orange corresponded to HCV gene targets, and red depicted the common targets shared by both.

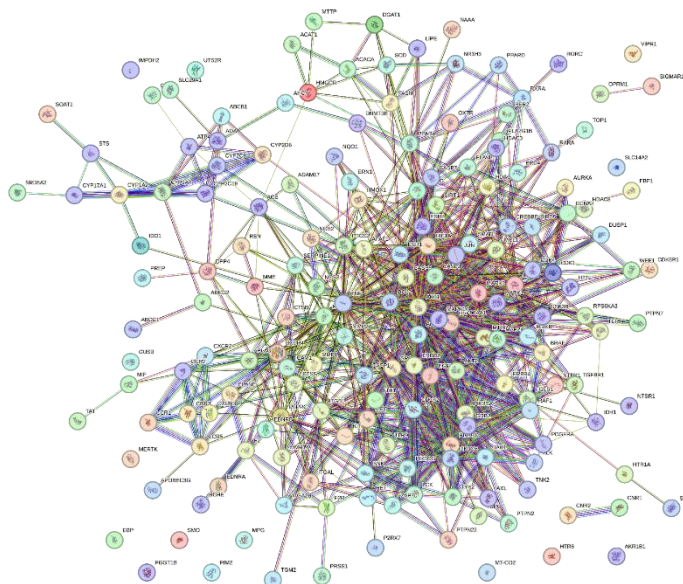


Figure 2: PPI network of AM and HCV targets.

In PPI network, nodes represented proteins, while edges (connecting lines) depicted their interactions. The analysis incorporated key network criteria, which included degree, such as the number of direct connections a node has, with higher values, indicating a more central and influential role in the network. Closeness Centrality measured how close a node was to others and was calculated as the inverse of the average shortest path distance. Higher values signified greater connectivity and faster communication with other nodes. Betweenness Centrality reflected the role of a node as a bridge in the network, revealing those that facilitated communication between other nodes

through the shortest paths. Proteins with the highest interaction counts were identified based on these criteria. Figure 3 depicted HCV-AM PPI network, and the top 11 proteins ranked by Degree, Closeness, and Betweenness Centrality were shown in Table 2.

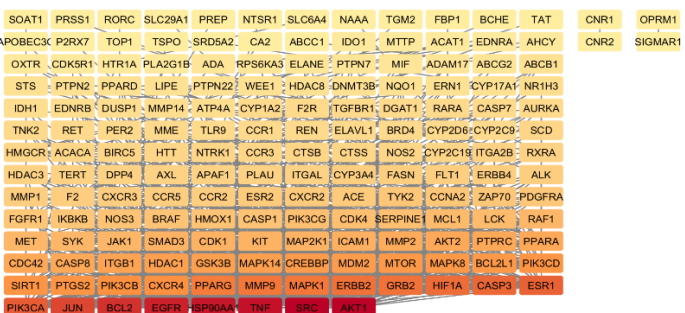


Figure 3: Visualization of HCV-AM PPI network. Nodes were color-coded, with more intense colors indicating genes with higher degrees of connectivity.

Core targets were identified using CytoHubba plug-in according to Degree, Betweenness, and Closeness Centrality values, as presented in Table 2. The top 11 targets were graphically represented in Figure 4. These targets included SRC, AKT1, TNF, HSP90AA1, EGFR, BCL2, JUN, PI3KCA, ESR1, CASP3, and HIF1A (Figure 4).

As shown in Table 2, the rankings of the 11 targets varied across Degree, Closeness, and Betweenness. To identify consistent core targets, the overlapping targets across these 3 metrics were analyzed, resulting in 5 key targets, namely SRC, AKT1, TNF, HSP90AA1, and ESR1. The combined results were visualized in Figure 4.

KEGG and GO analysis

Functional analysis using shinyGO 0.80 platform was conducted to explore KEGG pathways and GO categories, namely biological processes (BP), cellular components (CC), and molecular functions (MF). Statistically significant results (FDR/p < 0.05) were observed for 182 overlapping targets between AM and HCV.³⁰ Figure 5 displayed the top 10 enrichments for each category listed based on p-value.

Further analysis of the identified target genes was performed using GO and KEGG enrichment analysis. GO biological process enrichment emphasized the response to chemicals as the most significant process. The cellular component category identified the membrane raft and membrane microdomain as the top results. Furthermore, catalytic activity acting on a protein was the leading molecular function. KEGG pathway analysis revealed that the hepatitis C, PI3K-AKT signaling, and cancer pathways were among the enriched pathways significantly associated with HCV infection. Figure 5d showed the top 20 KEGG pathways, while Figure 6 visualized KEGG pathway of HCV, which indicated genes in the common target.

Molecular Docking

Based on the network pharmacology study, 11 core targets were identified, and the 5 best targets were selected, namely AKT1, SRC, tumor necrosis factor- α (TNF- α), HSP90AA1, and ESR1 for molecular docking. Furthermore, there were 12 compounds which each targeted AKT1 and TNF- α , such as Betaine, Avicenol A, Avicenol C, Avicenolone A, Avicenolone C, Avicenolone D, Avicenolone F, Avicenolone G, and Stenorpoquinone B. Those compounds except for Avicenolone D were also targeting HSP90AA1. Meanwhile, 2 compounds targeted SRC, namely Avicenol C and Avicenolone C, and 4 compounds targeted ESR1, including Betaine, Avicenolone C, Avicenolone A, and Avicenolone D. Each compound was docked to the corresponding protein target, and the results were shown in Table 3.

Binding energy of the native ligand (OXZ) to AKT1 was -5.726 kcal/mol, while binding energy of the compounds to AKT1 was in the range of -2.525 kcal/mol (for Betaine) and -7.074 kcal/mol (for Avicenolone D). Avicenolone D had a lower binding energy compared

to OXZ. Binding energy of the compounds to TNF- α was in the range of -2.512 kcal/mol and -6.585 kcal/mol, while the native ligand of TNF- α (307) was -5.287 kcal/mol. Compounds had lower binding energy than the native ligand (307), such as Avicenol A (-6.364), Avicenol C (-6.151 kcal/mol), Avicequinone A (-5.723 kcal/mol), Avicequinone C

(-5.929 kcal/mol), Avicennone A (-6.474 kcal/mol), Avicennone B (-6.585 kcal/mol), Avicennone C (-5.838 kcal/mol), Avicennone D (-5.282 kcal/mol), Avicennone F (-5.622 kcal/mol), Avicennone G (-6.321 kcal/mol), and Stenorpouquinone B (-6.030 kcal/mol).

Table 2: Top 11 proteins ranked by Degree, Closeness, and Betweenness Centrality.

Nama	Degree	Closeness	Betweenness
SRC	52	0.0818450847799891	0.5207667731629393
AKT1	52	0.06459061686821414	0.5224358974358975
TNF	49	0.15564144320655546	0.5292207792207793
HSP90AA1	48	0.0643204793746926	0.5109717868338558
EGFR	46	0.05668147287643477	0.5046439628482972
BCL2	43	0.05705247369730887	0.4969512195121951
JUN	39	0.03420439357540499	0.4909638554216868
PIK3CA	35	0.018373922758329504	0.4465753424657534
ESR1	34	0.09006988283195015	0.5062111801242236
CASP3	33	0.019109798822420466	0.45658263305322133
HIF1A	32	0.03653775947414212	0.48948948948948945

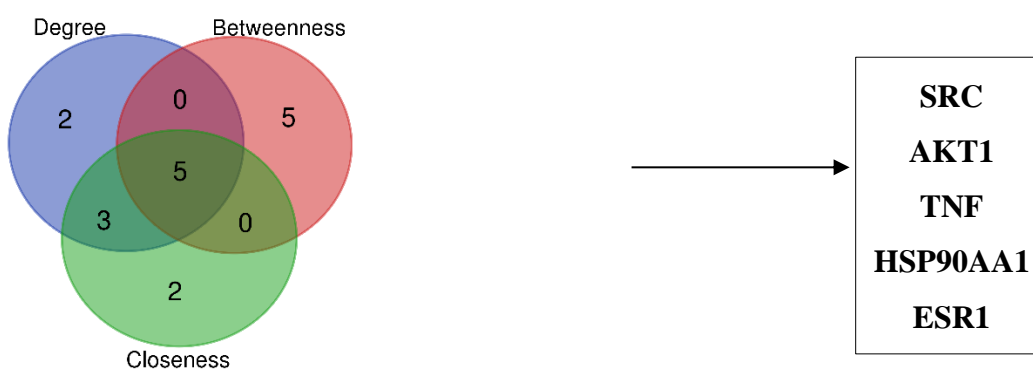


Figure 4: Combined targets based on Degree, Closeness, and Betweenness Centrality.

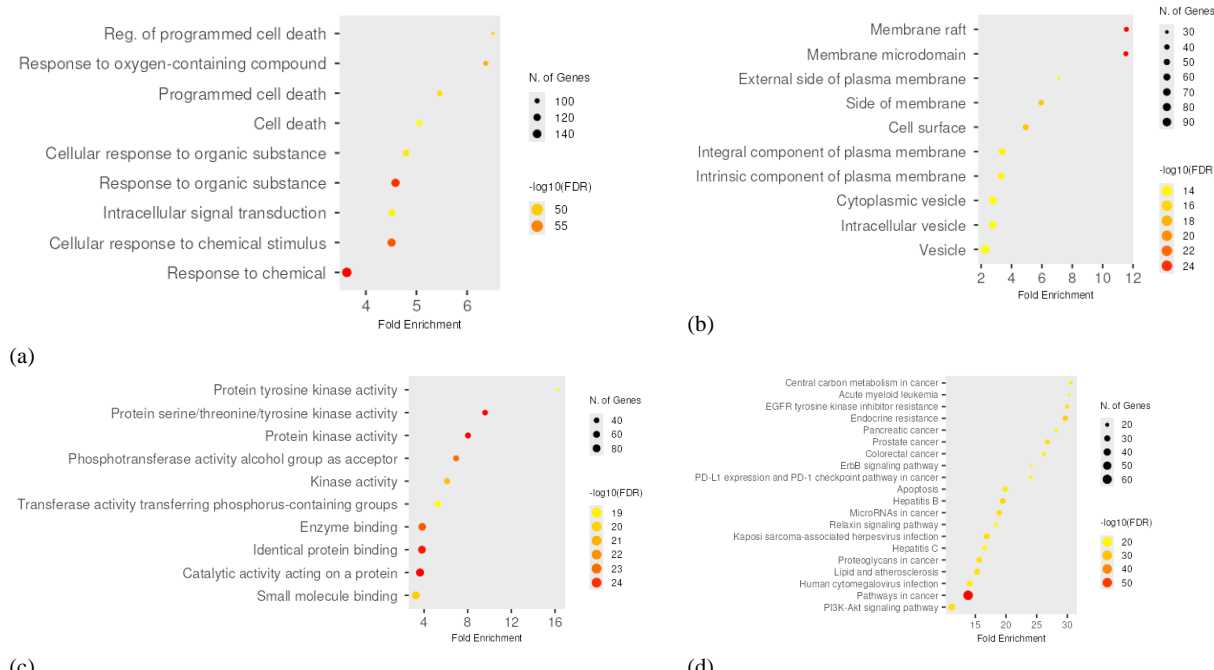


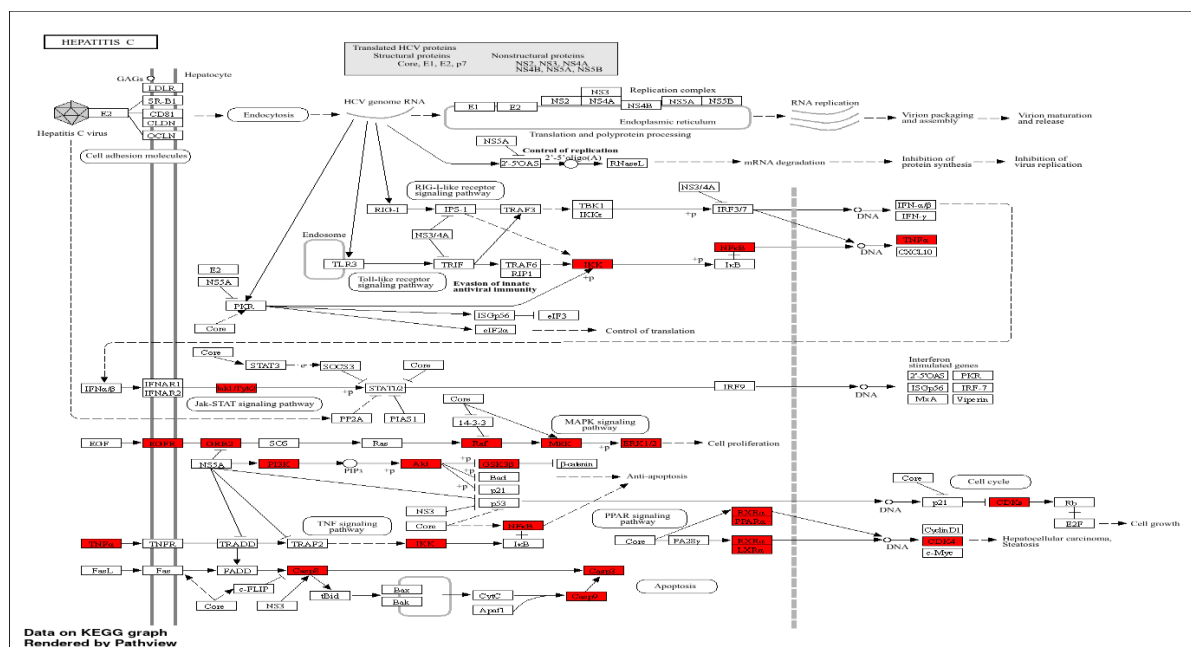
Figure 5: Diagram of enrichment analysis displaying results for (a) GO biological processes, (b) GO cellular components, (c) GO molecular functions, and (d) KEGG pathways.

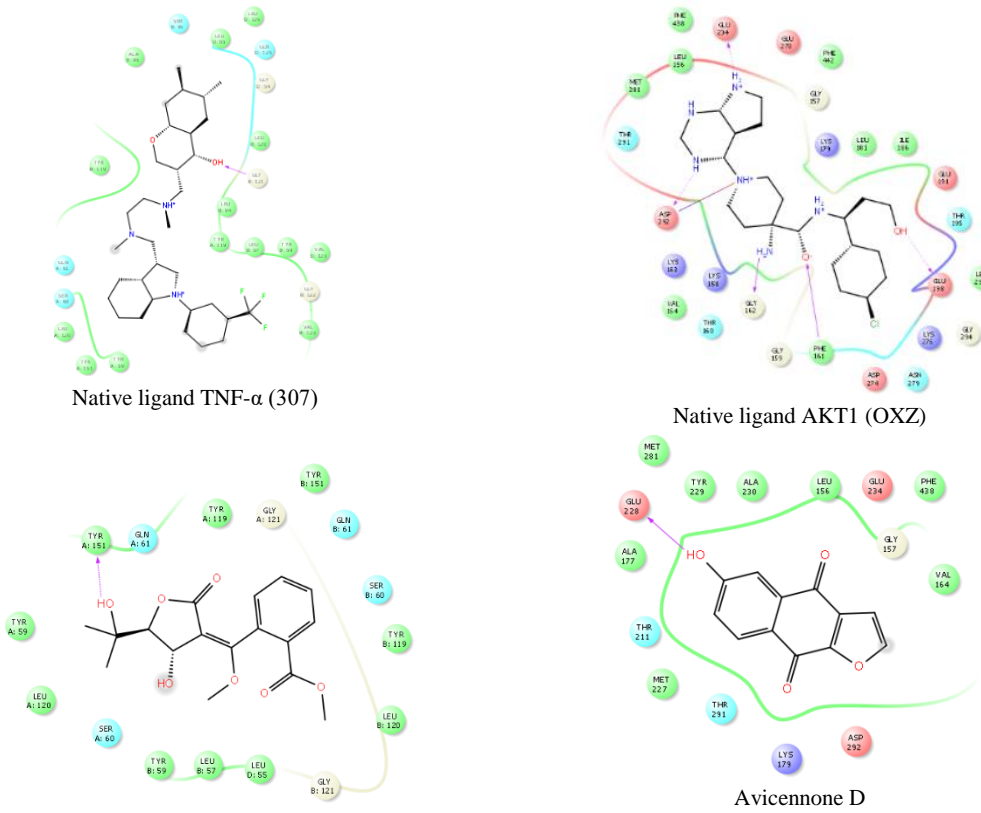
Table 3: Binding energy of each compound to its corresponding target.

Compound	Binding energy (kcal/mol)		TNF (PDB ID : 2AZ5)	HSP90AA1 (PDB ID : 3O0I)	ESR1 (PDB ID : 7UJY)
	AKT1 (PDB ID : 4GV1)	SRC (PDB ID : 1O43)			
Native ligand	-5.726 (OXZ)	-7.087 (821)	-5.287 (307)	-9.321 (P54)	-13.101 (RL4)
Betaine	-2.525		-2.512	-4.623	-2.305
Avicenol A	-4.217		-6.364	-7.711	
Avicenol C	-4.656	-3.381	-6.151	-10.369	
Avicequinone A	-3.635		-5.723	-8.393	
Avicequinone C	-4.292	-3.719	-5.929	-9.316	-6.784
Avicennone A	-3.753		-6.474	-8.027	-9.941
Avicennone B	-4.057		-6.585	-6.743	
Avicennone C	-4.032		-5.838	-7.783	
Avicennone D	-7.074		-5.282		-6.321
Avicennone F	-5.585		-5.622	-9.525	
Avicennone G	-4.725		-6.321	-7.793	
Stenopquinone B	-4.962		-6.030	-8.541	

In this study, the energies of the compounds to HSP90AA1 were in the range of -4.623 kcal/mol (for Betaine) and -10.369 kcal/mol (for Avicenol C), while the native ligand of HSP90AA1 (P54) was -9.321 kcal/mol. Notably, all compounds except for Betaine targeting HSP90AA1 exhibited binding energy comparable to those of that native ligand, and Avicenol C had a lower binding energy than that of the native ligand (P54). Meanwhile, binding energy of compounds to SRC and ESR1 was in the range of -3.381 kcal/mol (for Avicenol C) and -

3.719 kcal/mol (for Avicequinone C) for SRC, and -2.305 kcal/mol (for Betaine) and -9.941 kcal/mol (for Avicennone A) for ESR1, while binding energy of native ligand of SRC (821) and native ligand of ESR1 (RL4) was -7.087 kcal/mol and -13.101 kcal/mol. Figure 7 displayed the docked poses of Avicennone D and the native ligand to AKT1 and those of Avicennone B and the native ligand (307) to TNF- α , while Figure S1 displayed the remaining compounds to their corresponding targets.





Avicennone B
The docked poses to TNF- α : Native ligand (307, top) and
Avicennone B (bottom)
Figure 7: The docked poses of compounds and native ligand to AKT1 and TNF- α .

The pathophysiology of hepatitis C included viral infections that increased pro-inflammatory markers such as TNF- α as observed in patients with hepatocellular carcinoma (HCC).³⁴⁻³⁵ In chronic hepatitis C, TNF- α played a significant role in disease progression by promoting hepatocyte apoptosis and sustaining liver inflammation.³⁶ Patients with HCV infection exhibited elevated circulating levels of TNF- α , which correlated positively with the severity of liver disease.³⁷ In this study, compounds such as Avicenol A, Avicenol C, Avicequinone A, Avicequinone C, Avicennone A-G, and Stenopquinone B demonstrated stronger affinities for TNF- α compared to the reference compound, emphasizing their potential as TNF- α inhibitors. Avicenol A was previously reported to have cancer chemopreventive activity,³⁸ while Avicequinone C was reported to inhibit steroid 5 α -reductase.³⁹ Furthermore, Avicenol A and Avicennone G were reported to inhibit less in mitosis gene A-related kinase 2 (NEK2).⁴⁰ Moreover, AM extract suppressed the apoptotic pathway, thereby postponing the initiation of the catagen phase.⁴¹

Heat shock protein HSP90AA1 was a key cytosolic chaperone in eukaryotic cells and was responsible for assisting in the folding and assembly of newly synthesized and existing large peptide chains. HSP90AA1 also modulated a range of proteins, including transcription factors, kinases, E3 ubiquitin ligases, and tumor-promoting proteins. Eman A. Toraiha et al. (2019) reported significant upregulation of HSP90AA1 in the progression of HCV-induced hepatocellular carcinoma (HCC) and cirrhotic patients, with increased expression in advanced HCC stages.⁴² Similarly, Wu et al. (2021) emphasized the role of HSP90AA1 in the progression of HBV-related HCC and its correlation with patient survival in HCC.⁴³ In this study, 10 compounds were found to exhibit binding energy comparable to HSP90AA1, with Avicenol C and Avicennone F demonstrating lower binding energy than the native ligand (P54).

The docked poses to AKT1: Native ligand (OXZ, top),
Avicennone D (bottom)

Conclusion

In conclusion, this study explored the potential of AM to inhibit HCV infection. Through network pharmacology analysis, AM compounds were found to target key proteins such as SRC, AKT1, TNF, HSP90AA1, EGFR, BCL2, JUN, PI3KCA, ESR1, CASP3, and HIF1A. Molecular docking analysis revealed that Avicennone D exhibited a lower binding energy compared to the native ligands AKT1 and TNF- α . Similarly, Avicenol C and Avicennone F revealed lower binding energy than native ligands when bound to TNF- α and HSP90AA1, respectively. Additional compounds with reduced binding energy to TNF- α included Avicenol A, Avicenol C, Avicequinone A, Avicequinone C, Avicennone A-G, and Stenopquinone B. The integration of network pharmacology and molecular docking demonstrated that AM compounds had the potential to act on multiple targets in treating HCV infections. However, further study including experimental *in vitro* and *in vivo* assays was needed to support this result. These results suggested that AM could serve as a natural source for HCV inhibition.

Conflict of Interest

The authors declare no conflict of interest.

Authors' Declaration

The authors hereby declare that the work presented in this article is original and that any liability for claims relating to the content of this article will be borne by them.

Acknowledgments

The authors are grateful to Hibah Penelitian Fundamental Ministry of Education, Culture, Research, and Technology of Indonesia for funding this study with contract number: 20/UN29.20/PG/2024.

References

1. Hanafiah MK, Groeger J, Flaxman AD, Wiersma ST. Global epidemiology of hepatitis C virus infection: New estimates of age-specific antibody to HCV seroprevalence. *Hepatology*. 2013;57(4):1333-1342.
2. Mitra S, Naskar N, Lahiri S, Chaudhuri P. A study on phytochemical profiling of *Avicennia marina* mangrove leaves collected from Indian Sundarbans. *Sustain. Chem. Environ.* 2023;4:100041.
3. Wahyuni TS, Utsubo CA, Hotta H. Promising anti-hepatitis C virus compounds from natural resources. *Nat. Prod. Commun.* 2016;11(8):1193-1200.
4. Zandi K, Taherzadeh M, Tajbakhsh S, Yaghoubi R, Rastian Z, Sartavi K. Antiviral activity of *Avicennia marina* leaf extract on HSV-1 and vaccine strain of Polio virus in vero cells. *Int. J. Infect. Dis.* 2008;12:e298.
5. Lin C-K, Tseng C-K, Chen K-H, Wu S-H, Liaw C-C, Lee J-C. Betulinic acid exerts anti-hepatitis C virus activity via the suppression of NF- κ B- and MAPK-ERK1/2-mediated COX-2 expression. *Br. J. Pharmacol.* 2015;172(18):4481-4492.
6. Devi AS, Rajkumar J, Beenish TK. Detection of antibacterial compound of *Avicennia marina* against pathogens isolated from urinary tract infected patients. *Asian J. Chem.* 2014;26(2):458-460.
7. Behbahani M, Zadeh MS, Mohabatkar H. Evaluation of antitherapeutic activity of crude extract and fractions of *Avicenna marina*, in vitro. *Antiviral Res.* 2013;97(3):376-380.
8. Beula JM, Gnanadesigan M, Rajkumar PB, Ravikumar S, Anand M. Antiviral, antioxidant and toxicological evaluation of mangrove plant from South East coast of India. *Asian Pac. J. Trop. Biomed.* 2012;2(1, Supplement):S352-S357.
9. Kathiresan K. Chapter 8 - Bioprospecting potential of mangrove resources. In: Patra JK, Mishra RR, Thatoi H, editors. *Biotechnological Utilization of Mangrove Resources*: Academic Press; 2020. p. 225-241.
10. Premnathan M, Chandra K, Bajpai SK, Kathiresan K. A survey of some Indian marine plants for antiviral activity. *Bot. Mar.* 1992;35(4):321-324.
11. Luo H, Liu L, Zou J, Zhao J, Sun C, Ou S, Yang J. Network pharmacology study of *Seleromitrion diffusa* (Willd). R. J. Wang and *Scutellaria barbata* D. Don in the treatment of chronic atrophic gastritis. *Intell. Pharm.* 2024;2(1):45-50.
12. Liu T, Xin B, Zhang Q, Li T, Liu Y, Li L, Li Z. Exploring the molecular mechanism of Huangqin-Jinyinhua couplet medicines for the treatment of hand-foot and mouth disease using network pharmacology, molecular docking and bioinformatics databases. *Intell. Pharm.* 2023;1(2):106-115.
13. Xin B, Liu T, Wu Y, Hu Q, Dong X, Wang H, Li Z. Network pharmacological study of Banxia-Chenpi in the treatment of cough variant asthma in children with phlegm evil accumulation lung syndrome. *Intell. Pharm.* 2023;1(2):96-105.
14. Fitrianingsih AA, Santosaningsih D, Djajalaksana S, Muti, ah R, Lusida MI, Karyono SS, Prawiro SR. Network Pharmacology and In Silico Investigation on *Saussurea lappa* for Viral Respiratory Diseases. *Trop. J. Nat. Prod. Res.* 2024;8(1):5889-5896.
15. Tammu RM, Sitompul LR, Simamora R, Utomo DH, Putri ED. Revealing the Potential of New Immunomodulatory Agents from Katokkon Pepper as a Native Toraja Plant. *Trop. J. Nat. Prod. Res.* 2025;9(1):240-283.
16. Hadi S, Setiawan D, Komari N, Rahmadi A, Rahman A, Fansuri H, Nastiti K, Nisa K. Network Pharmacology and Docking of *Nephrolepis cordifolia* as Type-2 Antidiabetic Agent. *Trop. J. Nat. Prod. Res.* 2024;8(9):8345 – 8835.
17. Karima R, Elya B, Sauriasari R. Mechanism of Action of Glucomannan as a Potential Therapeutic Agent for Type 2 Diabetes Mellitus Based on Network Pharmacology and Molecular Docking Simulation. *Trop. J. Nat. Prod. Res.* 2023;7(12):5460-5469.
18. Daina A, Michielin O, Zoete V. SwissADME: a free web tool to evaluate pharmacokinetics, drug-likeness and medicinal chemistry friendliness of small molecules. *Sci. Rep.* 2017;7(1):42717.
19. Daina A, Michielin O, Zoete V. SwissTargetPrediction: updated data and new features for efficient prediction of protein targets of small molecules. *Nucleic Acids Res.* 2019;47(W1):W357-W364.
20. Keiser MJ, Roth BL, Armbruster BN, Ernsberger P, Irwin JJ, Shoichet BK. Relating protein pharmacology by ligand chemistry. *Nat. Biotechnol.* 2007;25(2):197-206.
21. Rebhan M, Chalifa-Caspi V, Prilusky J, Lancet D. GeneCards: a novel functional genomics compendium with automated data mining and query reformulation support. *Bioinformatics*. 1998;14(8):656-664.
22. Amberger JS, Bocchini CA, Schiettecatte F, Scott AF, Hamosh A. OMIM.org: Online Mendelian Inheritance in Man (OMIM®), an online catalog of human genes and genetic disorders. *Nucleic Acids Res.* 2015;43(D1):D789-D798.
23. Jiang L-R, Qin Y, Nong J-L, An H. Network pharmacology analysis of pharmacological mechanisms underlying the anti-type 2 diabetes mellitus effect of guava leaf. *Arab. J. Chem.* 2021;14(6):103143.
24. Shannon P, Markiel A, Ozier O, Baliga NS, Wang JT, Ramage D, Amin N, Schwikowski B, Ideker T. Cytoscape: A Software Environment for Integrated Models of Biomolecular Interaction Networks. *Genome Res.* 2003;13(11):2498-2504.
25. Kanehisa M, Furumichi M, Tanabe M, Sato Y, Morishima K. KEGG: new perspectives on genomes, pathways, diseases and drugs. *Nucleic Acids Res.* 2017;45(D1):D353-D361.
26. Zhou Y, Zhou B, Pache L, Chang M, Khodabakhshi AH, Tanaseichuk O, Benner C, Chanda SK. Metascape provides a biologist-oriented resource for the analysis of systems-level datasets. *Nat. Commun.* 2019;10(1):1523.
27. Ge SX, Jung D, Yao R. ShinyGO: a graphical gene-set enrichment tool for animals and plants. *Bioinformatics*. 2020;36(8):2628-2629.
28. Arba M, Wahyudi ST, Brunt DJ, Paradis N, Wu C. Mechanistic insight on the remdesivir binding to RNA-Dependent RNA polymerase (RdRp) of SARS-cov-2. *Comput. Biol. Med.* 2021;129:104156.
29. Sastry GM, Adzhigirey M, Day T, Annabhimoju R, Sherman W. Protein and ligand preparation: parameters, protocols, and influence on virtual screening enrichments. *J. Comput. Aided Mol. Des.* 2013;27(3):221-234.
30. Dong Q, Ren G, Li Y, Hao D. Network pharmacology analysis and experimental validation to explore the mechanism of kaempferol in the treatment of osteoporosis. *Sci. Rep.* 2024;14(1):7088.
31. Liu Z, Tian Y, Machida K, Lai MMC, Luo G, Foung SKH, Ou J-hJ. Transient Activation of the PI3K-AKT Pathway by Hepatitis C Virus to Enhance Viral Entry. *J. Biol. Chem.* 2012;287(50):41922-41930.
32. Lee W-P, Liao S-X, Huang Y-H, Hou M-C, Lan K-H. Akt1 is involved in HCV release by promoting endoplasmic reticulum-to-endosome transition of infectious virions. *Life Sci.* 2024;338:122412.
33. Han L, Huang X, Dahse H-M, Moellmann U, Fu H, Grabley S, Sattler I, Lin W. Unusual Naphthoquinone Derivatives from the Twigs of *Avicennia marina*. *J. Nat. Prod.* 2007;70(6):923-927.

34. Ali FEM, Abdel-Reheim MA, Hassanein EHM, Abd El-Aziz MK, Althagafy HS, Badran KSA. Exploring the potential of drug repurposing for liver diseases: A comprehensive study. *Life Sci.* 2024;347:122642.

35. Mourtzikou A, Alepaki M, Stamouli M, Pouliakis A, Skliris A, Karakitsos P. Evaluation of serum levels of IL-6, TNF- α , IL-10, IL-2 and IL-4 in patients with chronic hepatitis. *Immunología.* 2014;33(2):41-50.

36. Viganò M, Degasperi E, Aghemo A, Lampertico P, Colombo M. Anti-TNF drugs in patients with hepatitis B or C virus infection: safety and clinical management. *Expert Opin. Biol. Ther.* 2012;12(2):193-207.

37. Lee J, Tian Y, Chan ST, Kim JY, Cho C, Ou J-hJ. TNF- α induced by hepatitis C virus via TLR7 and TLR8 in hepatocytes supports interferon signaling via an autocrine mechanism. *PLoS Pathog.* 2015;11(5):e1004937.

38. Itoigawa M, Ito C, Tan HTW, Okuda M, Tokuda H, Nishino H, Furukawa H. Cancer chemopreventive activity of naphthoquinones and their analogs from *Avicennia* plants. *Cancer Lett.* 2001;174(2):135-139.

39. Karnsomwan W, Netcharoensirisuk P, Rungrothmongkol T, De-Eknamkul W, Chamni S. Synthesis, Biological Evaluation and Molecular Docking of Avicequinone C Analogues as Potential Steroid 5 α -Reductase Inhibitors. *Chem. Pharm. Bull. (Tokyo).* 2017;65(3):253-260.

40. Archana Vasuki K, Jemmy Christy H, Chandramohan V, Anand DA. Study of mangal based naphthoquinone derivatives anticancer potential towards chemo-resistance related Never in mitosis gene A-related kinase 2-In silico approach. *Mol. Simul.* 2021;47(13):1078-1092.

41. Prugsakij W, Numsawat S, Netcharoensirisuk P, Tengamnuay P, De-Eknamkul W. Mechanistic synergy of hair growth promotion by the *Avicennia marina* extract and its active constituent (avicequinone C) in dermal papilla cells isolated from androgenic alopecia patients. *PLoS One.* 2023;18(4):e0284853.

42. Toraih EA, Alrefai HG, Hussein MH, Helal GM, Khashana MS, Fawzy MS. Overexpression of heat shock protein HSP90AA1 and translocase of the outer mitochondrial membrane TOM34 in HCV-induced hepatocellular carcinoma: A pilot study. *Clin. Biochem.* 2019;63:10-17.

43. Wu Z, Wei C, Wang L, He L. Determining the Traditional Chinese Medicine (TCM) Syndrome with the Best Prognosis of HBV-Related HCC and Exploring the Related Mechanism Using Network Pharmacology. *Evid. Based Complement. Alternat. Med.* 2021;2021(1):9991533.